Journal of Human Evolution 172 (2022) 103256

Contents lists available at ScienceDirect

Journal of Human Evolution

journal homepage: www.elsevier.com/locate/jhevol

Morphological modularity in the anthropoid axial skeleton

Hyunwoo Jung [a, b, *], Noreen von Cramon-Taubadel [a]

[a] Buffalo Human Evolutionary Morphology Lab, Department of Anthropology, University at Buffalo, SUNY, 380 Academic Center, Ellicott Complex, Buffalo, NY 14261, USA
[b] Department of Anatomy, College of Graduate Studies, Midwestern University, 19555 N 59th Ave, Glendale, AZ 85308, USA

ARTICLE INFO

Article history:
Received 16 December 2021
Accepted 22 August 2022
Available online xxx

Keywords:
Morphological evolution
Hominoids
Hominins
Skull
Vertebrae

ABSTRACT

Previous research has found that hominoids have stronger modularity between limb elements than other anthropoids, suggesting that there is less constraint on morphological diversification (e.g., limb proportions) in hominoids in terms of evolutionary independence. However, degrees of modularity in the axial skeleton have not been investigated across a broad range of anthropoid taxa. Thus, it is unknown whether hominoids also have stronger modularity in the axial skeleton than other anthropoids, which has implications for the evolution of diverse torso morphologies in Miocene apes as well as the evolution of novel characteristics in the skull and vertebrae of fossil hominins. In this study, 12 anthropoid genera were sampled to examine degrees of modularity between axial skeletal elements (i.e., cranium, mandible, vertebrae, and sacrum). Covariance ratio coefficients were calculated using variance/covariance matrices of interlandmark distances for each axial skeletal element to evaluate degrees of modularity. The results showed that *Alouatta*, *Hylobates*, *Gorilla*, *Pan*, and *Homo* showed generally stronger modularity than other anthropoid taxa when considering all axial skeletal elements. When only considering the vertebral elements (i.e., vertebrae and sacrum), *Alouatta*, *Hylobates*, *Gorilla*, and *Pan* showed generally stronger modularity than other anthropoid taxa. Humans showed stronger modularity between the skull and vertebrae than other hominoids. Thus, the evolution of novel characteristics in the skull and vertebral column may have been less constrained in fossil hominins due to the dissociation of trait covariation between axial skeletal elements in hominoid ancestors, thus fostering more evolutionary independence between the skull and vertebral column.

1. Introduction

The study of morphological modularity among skeletal regions is important as modular structure can confine the effect of mutation or selection to limited sets of traits (Hallgrímsson et al., 2009; Armbruster et al., 2014; Goswami et al., 2014; Klingenberg, 2014), thus influencing the potential pathways of evolutionary change. Modular structure refers to higher interactions or correlation within skeletal regions (termed 'modules') with relatively less connectivity between-modules (Klingenberg, 2014). In other words, a modular structure suggests stronger within-module integration than between-module integration. As noted by Armbruster et al. (2014: 1), "integration and modularity refer to the patterns and processes of trait interaction and independence". In this regard, modularity and integration are not antonyms but complementary concepts. In the present study, modularity was used to refer to relative degrees of connectivity within and between a priori defined modules. Organisms with more modular body plans are considered to have different levels of within- and between-module constraints on morphological evolution as modules tend to have greater evolutionary independence compared with other body regions. Therefore, trait covariation may have to be dissociated or structured in differential ways to facilitate the evolution of novel skeletal morphology (Armbruster et al., 2014; Goswami et al., 2014; Klingenberg, 2014). For instance, Young et al. (2010) reported that hominoids have stronger degrees of modularity (i.e., lower covariation) between limb elements than other anthropoids. Thus, Young et al. (2010) suggested that there was dissociation of trait covariation between limb elements in hominoid ancestors, which allowed for the evolution of novel limb proportions among hominoids, including the human lineage in relation to obligate bipedal locomotion (i.e., short forelimbs and long hindlimbs).

* Corresponding author.
E-mail address: hjung@midwestern.edu (H. Jung).

https://doi.org/10.1016/j.jhevol.2022.103256
0047-2484/

In the vertebral column, the results of Williams et al. (2019) suggest that antipronograde and dorsostable hominoids may have experienced reduced biomechanical and developmental/genetic constraints compared to pronograde and dorsomobile anthropoids in terms of the number of presacral vertebrae. Although the axial skeleton is traditionally separated into the vertebral column and the skull, it is important to note that the basicranium shares developmental origins and genetic pathways with vertebral elements (Burke et al., 1995; Wellik, 2007) and acts as the 'central integrator' of the skull (Lieberman, 2011), suggesting the existence of modular structure across the skull and vertebral column. However, despite its importance for understanding the evolutionary history of the human and nonhuman primate bauplan, only a few studies have investigated modularity (or covariation) among axial skeletal elements in primates (e.g., Villamil, 2018; Arlegi et al., 2018, 2020, 2022; Villamil and Santiago-Nazario, 2021). Moreover, these studies have tended to focus on limited axial skeletal regions, such as the cranium and/or cervical vertebrae, and only examined morphological integration/modularity in hominoids (Villamil, 2018; Arlegi et al., 2018, 2022; Villamil and Santiago-Nazario, 2021). Although Arlegi et al. (2020) investigated covariation across almost all vertebrae, the analyses were limited to humans. Thus, it is unknown whether axial skeletal elements of hominoids also have stronger degrees of modularity than other anthropoids as has been found to be the case for limb elements (Young et al., 2010). Knowing this is important as it may suggest that hominoid ancestors had weaker genetic constraints among traits or lower evolutionary constraint (i.e., constraint on the evolution of diverse torso morphology in response to diverse locomotor repertoires) than other anthropoid groups, thus allowing for the evolution of novel axial skeletal morphologies in the hominoid lineage, including the unique skeletal morphology associated with human bipedalism.

It is well understood that humans display novel characteristics in the skull (Lieberman, 2011; Gómez-Robles et al., 2017; Schroeder and von Cramon-Taubadel, 2017; Veneziano et al., 2018; von Cramon-Taubadel et al., 2021) and vertebrae (Latimer and Ward, 1993; Shapiro, 1993a; Been et al., 2019) related to our upright body posture and bipedal form of locomotion. For instance, Schroeder and von Cramon-Taubadel (2017) found that humans showed a strong signal of directional selection on basicranial flexion, facial retraction, and cranial vault expansion among ape lineages. Directional selection for brain expansion may have been one of the major forces that shaped human skull morphology, given that facial retraction is also associated with basicranial flexion and brain size expansion (Lieberman et al., 2000; Lieberman, 2011; Neaux et al., 2018). In terms of the vertebral column, there is a mosaic of primitive and novel characteristics observable among australopiths (Johanson et al., 1982; Lovejoy et al., 1982; Shapiro, 1993b; Meyer et al., 2015, 2017; Williams et al., 2018; Williams and Meyer, 2019) and fossil *Homo* specimens (Latimer and Ward, 1993; Meyer, 2005; Gómez-Olivencia et al., 2013, 2017; Arsuaga et al., 2015; Williams et al., 2017; Meyer and Williams, 2019; Gómez-Olivencia and Been, 2019). Although australopiths show more primitive vertebral morphologies than early and late *Homo* specimens, australopiths have certain degrees of lumbar lordosis, which is thought to be an adaptation for bipedal locomotion to move the center of the torso over the sacroiliac and the hip joints (Latimer and Ward, 1993; Shapiro, 1993a,b; Gómez-Olivencia and Been, 2019; Meyer and Williams, 2019; Williams and Meyer, 2019; Williams et al., 2021). Also, early and late *Homo* specimens showed lumbar lordosis although the Sima de los Huesos (SH) *Homo* specimens and Neanderthals had lesser degrees of lumbar lordosis than modern humans (Latimer and Ward, 1993; Gómez-Olivencia et al., 2013; Gómez-Olivencia and Been, 2019; Meyer and Williams, 2019; but see Williams et al., 2022). Taken together, the evolution of the novel characteristics and morphological diversification in the skull and vertebral column of hominins suggest that a high evolutionary potential may have pre-existed in hominoid ancestors and/or that the human lineage presents very different patterns of modularity compared with other hominoids.

In this regard, the purpose of the present study was to investigate both whether hominoids have relatively stronger modularity (i.e., weaker covariation) among axial skeletal elements than other anthropoids and to compare patterns of modularity between humans and other hominoids, by testing the following two hypotheses: 1) hominoids will have stronger degrees of modularity between axial skeletal elements (i.e., cranium, mandible, vertebrae, and sacrum) than other anthropoids as was previously reported to be the case for limb elements (Young et al., 2010); 2) humans will have different patterns of modularity in the axial skeleton compared to other hominoids.

2. Materials and methods

2.1. Skeletal materials

For this study, major anthropoid taxa were examined at the genus level (Table 1; Supplementary Online Material [SOM] Table 1). When possible, a single species within each genus was sampled. Individuals were selected if there were identifiable landmarks on the cranium, mandible, five cervical vertebrae, five thoracic vertebrae, three lumbar vertebrae, and sacrum. The skull (i.e., cranium and mandible) directly interacts with the cervical vertebrae to generate head and neck movements and create balance (Lieberman, 2011). Moreover, the basicranium shares developmental origins (i.e., somite differentiation and segregation) and genetic pathways (i.e., Hox gene family) with vertebral elements (Burke et al., 1995; Wellik, 2007; Lieberman, 2011). Thus, the skull is included in the analyses as it shares functional demands and developmental pathways with the vertebral column. However, analyses were also repeated just using the vertebral elements (vertebrae and sacrum), given that the cranium and mandible also form a distinct functional module (related to feeding, cognition, and sensory function) separate from the vertebral column. Three-dimensional surface scans of skull and vertebral elements were generated using an HDI-120 and a Macro R5X structured-light scanner (LMI technologies Inc., Vancouver, Canada). In this study,

Table 1
Sample description and individual variation controlled for by mean centering.

Taxa	Sex			Controlled variation
	Male	Female	Total	
Alouatta palliata	7	3	10	S, SP, T, L, SAC
Alouatta caraya	3	3	6	
Cercopithecus ascanius	9	6	15	S, SP, T, L
Cercopithecus mitis	8	7	15	
Chlorocebus aethiops	11	9	20	S, SP, WC, T, L
Chlorocebus pygerythrus	6	6	12	
Colobus guereza	8	0	8	None
Gorilla gorilla	6	5	11	S, L, SAC
Homo sapiens	48	38	86	S
Hylobates lar	22	23	45	S, L, SAC
Lophocebus albigena	4	4	8	S
Macaca fascicularis	22	17	39	S, WC, T, L
Pan troglodytes	16	15	31	S, T, L, SAC
Pongo pygmaeus	5	3	8	S, SAC
Sapajus apella	10	2	12	S

Abbreviations: S = sex; SP = species; WC = wild vs. captive; T = identity of the last thoracic vertebra; L = identity of the last lumbar vertebra; SAC = the number of sacral vertebrae.

adult specimens were used and adult status was evaluated by observation of a (fully) fused spheno-occipital synchondrosis and/or the third molar on the occlusal surface. Variation attributable to sex, species, wild vs. captive, identity of the last thoracic or lumbar vertebrae, and/or the number of sacral vertebrae was controlled by mean centering within each genus (Table 1; Jung et al., 2021). Mean centering was conducted by subtracting a variable's mean from all observations in the data, which standardizes all variable means to zero (Iacobucci et al., 2016).

In the vertebral column, five cervical, five thoracic, three lumbar vertebrae, and the sacrum were selected as representative samples of the vertebral column, as vertebral elements share developmental origins and genetic control across taxa (Burke et al., 1995; Wellik, 2007), and functional roles within vertebral regions (Shapiro; 1993a; Been et al., 2019). Thus, a partial vertebral column was used as a proxy for the entire vertebral column to calculate degrees of modularity in this study, given that taxa (and in some cases, individuals within taxa) vary in the absolute number of vertebrate elements they possess. For the cervical vertebrae, the first, second, third, fifth, and seventh (C1, C2, C3, C5, and C7) were sampled as all primates have seven cervical vertebrae. For the thoracic vertebrae, the first, fourth, seventh, tenth, and twelfth/thirteenth (T1, T4, T7, T10, and T12/13) were sampled in catarrhines and the first, fifth, eighth, twelfth, and fourteenth/fifteenth (T1, T5, T8, T12, and T14/15) were sampled in platyrrhines. Thus, the selected thoracic vertebrae included the first and last thoracic vertebrae in all cases, plus the vertebra halfway along the thoracic spine (T7 or T8), and two vertebrae approximately equidistance between the last thoracic vertebra and the midpoint (T4/T5 and T10/T12). This sampling strategy allows for a relatively constant interval coverage in the thoracic region. For the lumbar vertebrae, the first, 'middle,' and last lumbar vertebrae were sampled. For instance, the sampled lumbar vertebrae were first, third, and fourth/fifth (L1, L3, and L4/5) in *Alouatta*, first, third, and fifth (L1, L3, and L5) in *Sapajus* and *Homo*, first, fourth, sixth/seventh (L1, L4, L6/7) in *Colobus*, *Cercopithecus*, *Chlorocebus*, *Lophocebus*, and *Macaca*, first, third, and fifth/sixth (L1, L3, L5/6) in *Hylobates*, first, third, and forth (L1, L3, and L4) in *Pongo*, and first, second, third/fourth (L1, L2, L3/4) in *Pan* and *Gorilla*. Thoracic vertebrae were defined as rib-bearing vertebrae, whereas lumbar vertebrae were defined as non–rib-bearing vertebrae caudal to thoracic vertebrae in the thoracolumbar region (Williams et al., 2016). This criterion was chosen as the last rib-bearing vertebra in some anthropoid taxa (e.g., cercopithecoids) is often not in the same level as the transitional (or 'diaphragmatic') vertebra, which have coronally oriented prezygapophyseal articular facets and obliquely or sagittally oriented postzygapophyseal articular facets (Williams et al., 2016).

The condition of fused coccygeal vertebrae to the sacrum was assessed based on the cornua morphology of the sacrum and coccygeal vertebrae, which projects inferiorly and superiorly, respectively (Russo and Williams, 2015). Moreover, as Russo and Williams (2015) reported, humans also have the apex and base of the sacral hiatus mostly located at the penultimate sacral vertebrae and at the ultimate sacral vertebra, respectively. These criteria were considered when counting the number of sacral vertebrae and placing landmarks on the sacrum.

2.2. Landmarking protocol

Landmarks were digitized on the left side of skeletal elements using the software Landmark v. 3.0.0.6 (Wiley et al., 2005; Fig. 1; SOM Tables S2–S7). When the left side was damaged, the right side was landmarked. In specimens with significant sagittal and nuchal crests, the average midline point of the left and right side of the crest at the level of the vault was used to estimate the position of midline landmarks bregma and lambda. When the spinous process in cervical vertebrae was bifurcated, the average coordinates between the left and right sides of the bituberculosity were used. When there was only one costal facet in the last rib-bearing vertebra, the left side was landmarked unless there was bilateral asymmetry on the vertebral body. The side with the costal facet was landmarked when there was marked asymmetry. There was a partially sacralized last lumbar vertebra in one orangutan, one chimpanzee, and two humans. In these specimens, the last lumbar vertebra could be disarticulated as the impacted side was slightly or moderately sacralized. On partially sacralized last lumbar vertebrae, the left side was landmarked unless there was marked bilateral asymmetry. The side without partial sacralization was landmarked when there was marked asymmetry.

Intraobserver error was evaluated by calculating standard deviations among coordinates on 3D models. The cranium, mandible, C1, C2, T7, and sacrum of one male *Macaca fascicularis* were digitized three times as each scan shares the same fixed coordinate plane (von Cramon-Taubadel et al., 2007). The mean measurement error was 0.261 mm in the cranium, 0.135 mm in the mandible, 0.045 mm in C1, 0.056 mm in C2, 0.081 mm in T7, and 0.107 mm in the sacrum (SOM Tables S2–S7).

2.3. Analytical methods

The covariance ratio coefficient (CR) was used to calculate degrees of modularity as it is insensitive to sample size or number of variables (Adams, 2016). To calculate the CR, the variance/covariance (V/CV) matrix needs to be structured as follows (Adams, 2016):

$$S = \begin{bmatrix} S_{11} & S_{12} \\ S_{21} & S_{22} \end{bmatrix}$$

where S_{11} is the within-module V/CV matrix for module 1, S_{22} is the within-module V/CV matrix for module 2, and S_{12} or S_{21} is the between-module V/CV matrix for modules 1 and 2 (Adams, 2016). Matrix S has p + q dimensions when module 1 and module 2 have p and q number of traits, respectively. Then, the calculation of the CR is as follows, which presents covariance ratio between two blocks (Adams 2016):

$$CR = \sqrt{\frac{\text{trace}(S_{12}S_{21})}{\sqrt{\text{trace}(S^*_{11}S^*_{11})\text{trace}(S^*_{22}S^*_{22})}}}$$

where S^*_{11} and S^*_{22} are the covariance matrices within modules with zeros in the diagonal elements. Trace $(S^*_{11}S^*_{11})$ or trace $(S^*_{11}S^*_{11})$ refers to the sum of the squared covariance in each block (within-modules), whereas trace $(S_{12}S_{21})$ is the sum of the squared covariance between two modules as diagonal elements are excluded (Adams, 2016). The covariance ratio coefficient can be larger than 1 when covariation between modules is larger than covariation within modules. A CR value of 1 or more indicates no modularity, whereas a CR value of 0 means complete modularity between modules (Adams, 2016). Thus, a lower CR value indicates stronger degrees of modularity (i.e., high levels of within-module covariation and little/no covariation between modules). V/CV matrices were generated using all possible Euclidean interlandmark distances for a given skeletal element to calculate CR. The covariance coefficient ratio was calculated using the 'modularity.test' function in the 'geomorph' package v. 3.2.1 (Adams and Otárola-Castillo, 2013) in R v. 3.6.3 (R Core Team, 2020). One axial skeletal element was assigned to block 1 and another one was

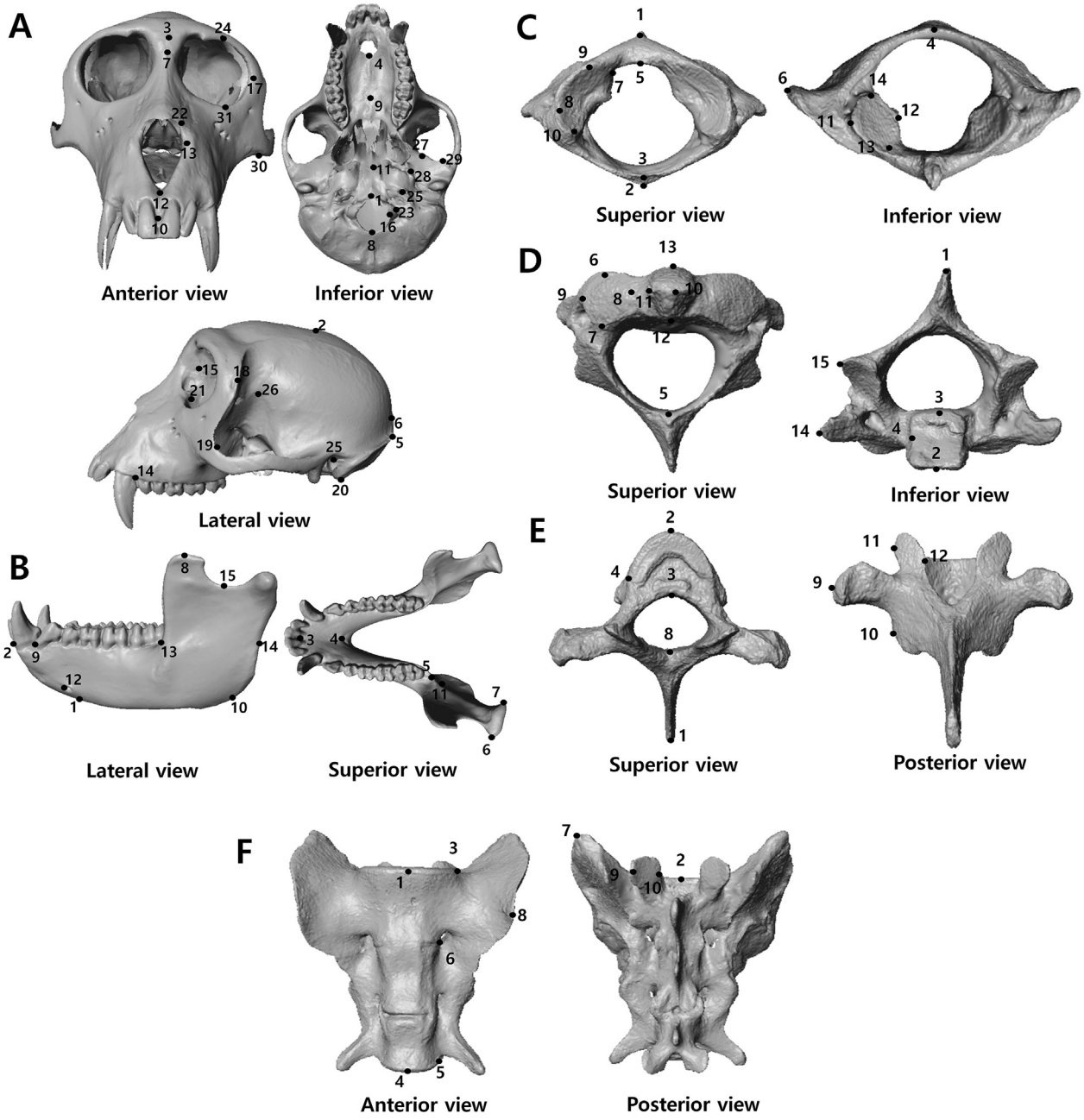

Figure 1. Landmarks used in this study placed on the cranium (A), mandible (B), first cervical vertebra (C), second cervical vertebra (D), seventh thoracic vertebra (E), and sacrum (F). The landmarks are essentially the same for all thoracic and lumbar vertebrae (for details, see SOM Tables S2–S7).

assigned to block 2 in the aforementioned CR formula to calculate CR values between all possible pairs of axial skeletal elements.

Mann–Whitney U tests were conducted using 'wilcox.test' function in R to statistically compare mean CR values in the axial skeletal elements or in the vertebral elements among anthropoid taxa with Bonferroni correction (i.e., statistically significant when $p < 0.00076$ for 66 Mann–Whitney U tests in anthropoids; $p < 0.005$ for 10 Mann–Whitney U tests in hominoids). Mann–Whitney U tests were used as distributions of CR values were not normal ($p < 0.05$) in most anthropoid taxa when tested using the 'shapiro.test' function in R.

Visual inspection of heatmaps was used to examine the overall pattern of CR in all possible pairs of axial skeletal elements for each taxon. A heatmap was generated by using 'corrplot' function in 'corrplot' package v. 0.92 (Wei et al., 2017) in R. Elements in heatmaps represent relative CR values between pairs of axial skeletal elements. Light and dark blue color shows relatively lower or higher CR values, respectively. Lastly, to quantify which taxa were most similar and different from each other in terms of patterns of CR values, pairwise Euclidean distances were calculated between taxon heatmap matrices using element-wise subtractions. To visualize these patterns of similarity and difference, distance matrices representing pairwise differences in the degrees of modularity (i.e., CR values) were subjected to 2D nonmetric multidimensional scaling (MDS) analysis using PAST v. 3 (Hammer et al., 2001), such that dissimilarities between heatmaps could be represented and visualized in two dimensions (Groenen and van de Velden, 2005). In each 2D MDS plot, 'stress' values were reported to

quantify the degree of correspondence between the original and projected distance matrices (Groenen and van de Velden, 2005). The stress value is a goodness-of-fit statistic (i.e., how well the inputted distance matrix can be rendered in two dimensions) and ranges between 0 and 1 (Groenen and van de Velden, 2005). Thus, low stress values indicate a better representation of the original distance matrix in two dimensions.

3. Results

Hominoids generally showed lower CR (i.e., stronger modularity) than other anthropoid taxa with some exceptions (Fig. 2; Table 2). The mean CR between axial skeletal elements or between vertebral elements (i.e., vertebrae and sacrum) was highest in *Macaca* and lowest in *Pan* (Fig. 2; Table 2). In the axial skeleton, *Alouatta*, *Hylobates*, *Gorilla*, *Pan*, and *Homo* showed generally lower CR than other taxa in the axial skeletal elements (Fig. 2; Table 2; SOM Table S8). Of the hominoid taxa, *Pongo* had the highest CR among hominoids for both the axial skeleton and vertebral elements. In the vertebral elements, *Alouatta*, *Hylobates*, *Gorilla*, and *Pan* showed generally lower CR than other taxa (Fig. 2; Table 2; SOM Table S9).

In *Homo*, the mean CR between skull elements (i.e., cranium and mandible) and vertebral elements (i.e., vertebrae and sacrum) was significantly lower than other hominoids (Fig. 3; SOM Table S10). It is worth noting that the use of a highly conservative alpha-level applied during Bonferroni correction of the Mann–Whitney U tests may increase the likelihood of Type-II errors (i.e., false negatives), and as such the Mann–Whitney U test results should be assessed with some caution. Nevertheless, the overall patterns of modularity among taxa remain the same regardless of the precise statistical cut-off points suggested by the results of the Mann–Whitney U test results.

Looking at the heatmap results, it seems that *Homo* showed more evenly patterned CR in the vertebral elements and stronger modularity between the skull and vertebral column compared to other hominoids (Fig. 3). In addition, the CR was relatively high in the cervical region for *Alouatta*, *Colobus*, and *Macaca*, in the thoracic region for *Chlorocebus*, *Hylobates*, *Pan*, and *Homo*, and in the lumbar region for *Sapajus*, *Cercopithecus*, *Lophocebus*, *Pongo*, and *Gorilla* (Fig. 3; SOM Tables S11–S22). Moreover, the patterns of CR displayed by the heatmaps were also not consistent even in taxa with high CR in similar vertebral region. Thus, there was no detectable pattern suggesting whether there is a consistently more modular vertebral region across anthropoids in general.

In the 2D MDS plots of the taxon pairwise distances between CR heatmaps (Figs. 4 and 5), hominoids were generally separated from other catarrhines (i.e., cercopithecoids) along the first axis, reflecting the systematic differences in their levels of axial skeletal modularity seen in the results of mean and pairwise CR values (Figs. 2 and 3; Table 2). However, it should be noted that, with respect to all axial skeletal elements, *Pongo* represents an exception to this general pattern in not being clustered with other hominoids (Fig. 4). However, in the case of vertebral elements, *Pongo* was clustered with other hominoid taxa. In the case of the more distantly related platyrrhine taxa, *Alouatta* was situated closer to hominoids, reflecting their relatively lower CR values, whereas *Sapajus* was closer to cercopithecoids in the 2D MDS plots, consistent with their elevated CR values (i.e., weaker modularity).

4. Discussion

4.1. Comparison between hominoids and other anthropoids

The results partially supported the first hypothesis of the present study. Hominoids showed generally stronger degrees of modularity (i.e., lower CR) between axial skeletal elements and/or between vertebral elements than other anthropoid taxa, although there were some exceptions (Fig. 2; Table 2; SOM Tables S8 and S9). *Pongo* had overall higher CR than most other hominoid taxa for the whole axial skeleton, although this was not the case for the vertebral elements, whereas *Alouatta* had lower CR than other nonhominoid taxa and displayed CR levels in the hominoid range. Moreover, it should be noted that *Pongo* was not clustered with other hominoids when considering all axial skeletal elements in the 2D MDS plot (Fig. 4), which may be due to its small sample size. However, *Lophocebus* and *Colobus* were clustered with other cercopithecoids although they also had the same small sample size as *Pongo*. More importantly, the CR is generally considered insensitive to sample size (Adams, 2016). Thus, there is currently no clear explanation for the separation of *Pongo* from other suspensory hominoids in terms of CR for the whole axial skeleton.

Young et al. (2010) also reported that hominoids have relatively stronger degrees of modularity between limb elements than other

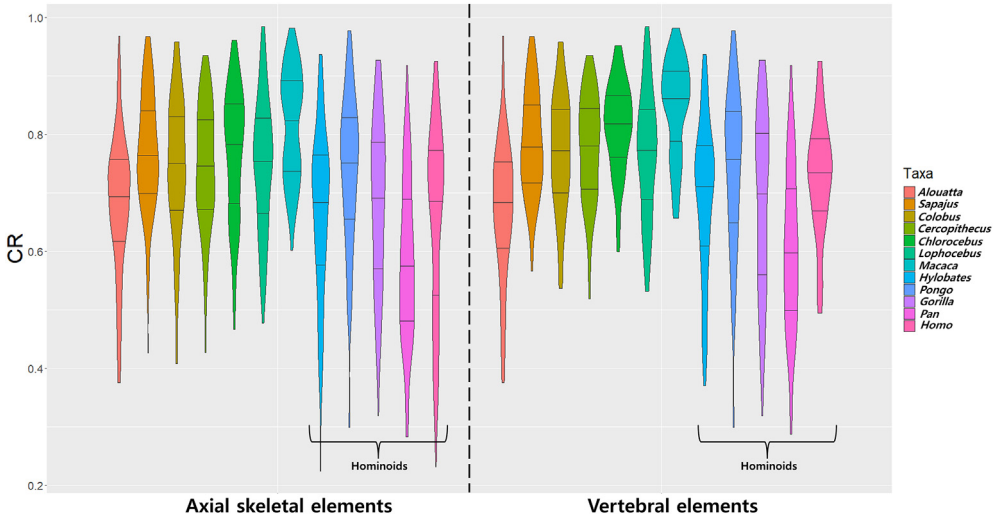

Figure 2. Covariance ratio coefficient (CR) in the axial skeletal elements and vertebral elements. Horizontal lines inside violin plot present 25%, 50%, and 75% quartiles based on the density estimate.

Table 2
Mean covariance coefficient ratio (CR) in axial skeletal elements and vertebral elements with standard deviation in parenthesis. The taxa are ordered from highest to lowest mean CR in the axial skeletal elements.

Taxa	Axial	Significantly different taxa in axial[a]	Vert	Significantly different taxa in vert
Macaca	0.816 (0.093)	H: none L: all taxa except Ch	0.845 (0.084)	H: none L: all taxa except Ch
Sapajus	0.770 (0.101)	H: Ma L: Al, Go, Ho, Hy, Pa	0.786 (0.089)	H: Ma L: Al, Go, Ho, Hy, Pa
Chlorocebus	0.769 (0.112)	H: none L: Al, Go, Ho, Hy, Pa	0.813 (0.077)	H: none L: Al, Go, Ho, Hy, Pa, Po
Colobus	0.748 (0.116)	H: Ma L: Al, Go, Ho, Hy, Pa	0.769 (0.101)	H: Ma L: Al, Hy, Pa
Lophocebus	0.748 (0.113)	H: Ma L: Al, Go, Ho, Hy, Pa	0.767 (0.108)	H: Ma L: Al, Hy, Pa
Cercopithecus	0.746 (0.105)	H: Ma L: Al, Ho, Hy, Pa	0.775 (0.092)	H: Ma L: Al, Go, Hy, Pa
Pongo	0.738 (0.130)	H: Ma L: Al, Ho, Hy, Pa	0.741 (0.138)	H: Ch, Ma L: Al, Pa
Gorilla	0.684 (0.141)	H: Ch, Co, Lo, Ma, Sa L: Pa	0.689 (0.152)	H: Ce, Ch, Ma, Sa L: Pa
Alouatta	0.679 (0.119)	H: Ce, Ch, Co, Lo, Ma, Po, Sa L: Pa	0.671 (0.118)	H: Ce, Ch, Co, Lo, Ma, Po, Sa L: Pa
Hylobates	0.668 (0.140)	H: Ce, Ch, Co, Lo, Ma, Po, Sa L: Pa	0.692 (0.132)	H: Ce, Ch, Co, Lo, Ma, Sa L: Pa
Homo	0.654 (0.162)	H: Ce, Ch, Co, Lo, Ma, Po, Sa L: Pa	0.727 (0.098)	H: Ch, Ma, Sa L: Pa
Pan	0.584 (0.138)	H: all taxa L: none	0.603 (0.137)	H: all taxa L: none

Abbreviations: axial = axial skeletal elements; vert = vertebral elements; H = taxa with significantly higher CR; L = taxa with significantly lower CR; Al = *Alouatta*; Ce = *Cercopithecus*; Ch = *Chlorocebus*; Co = *Colobus*; Go = *Gorilla*; Ho = *Homo*; Hy = *Hylobates*; Lo = *Lophocebus*; Ma = *Macaca*; Pa = *Pan*; Po = *Pongo*; Sa = *Sapajus*.
[a] Significant result when $p < 0.00076$ following Bonferroni correction.

anthropoids, which is assumed to reflect the more limited effects of mutation or selection on certain skeletal elements (Klingenberg, 2014). Thus, the results suggest that hominoids have weaker genetic constraints among traits or lower evolutionary constraints on morphological diversification in the axial skeleton, similar to what was observed among limb elements (Young et al., 2010), as a result of this overall lower between-module covariation (Klingenberg, 2014). As limb elements and vertebrae share similar Hox gene expression domains (Wellik, 2007; Rolian, 2014), dissociation among vertebral elements and among limb segments may be related to analogous developmental mechanisms and resultant reduction of constraint on morphological evolution in hominoids. Hence, stronger degrees of modularity in hominoids may be related to the evolution of diverse torso and limb morphologies in response to variable locomotor repertoires found across Miocene apes (Ward, 2015; Pilbeam and Lieberman, 2017).

No vertebral region was found to show consistently higher or lower CR across all anthropoid taxa studied here, and the differences in patterns of modularity seen in the heatmaps (Fig. 3) did not fall along strict phylogenetic or taxonomic lines. Arlegi et al. (2020) reported relatively stronger covariation among modern human thoracic vertebrae when compared with cervical and lumbar vertebrae, which was inferred to reflect either the notion that the thoracic region is the first module to evolve in the mammalian vertebral column (Jones et al., 2018) or is associated with the need for greater stability in the thoracic region as a result of bipedalism. Here, we also found strong covariation in the thoracic region of humans (Fig. 3), consistent with the results of Arlegi et al. (2020). However, most anthropoid taxa (eight out of 12 genera analyzed here) showed relatively stronger covariation in either the cervical or lumbar regions and not in the thoracic region (Fig. 3). Moreover, felids did not show stronger covariation in the thoracic region compared with the cervical and lumbar regions (Randau and Goswami, 2017). Thus, taken together, these results suggest that the strong covariation in the thoracic region found in modern humans here and by Arlegi et al. (2020) is not indicative of a universal mammalian pattern due to the early evolution of the mammalian thoracic region. Also, the results presented here do not suggest that the relatively high modularity of the thoracic region in humans reflects the need for greater stability during bipedal locomotion, as *Chlorocebus*, *Hylobates*, and *Pan* also showed strong covariation in the thoracic region in this study. Thus, the patterns of CR in the vertebral column may not be strictly related to posture or locomotion. Still, it is possible that some other factor is contributing toward the functional/developmental modularization of the thoracic vertebral region. Alternatively, the results might instead reflect random processes (e.g., drift) in major anthropoid taxa. Further studies focused on broader taxonomic groups representing various locomotor behaviors (e.g., bipedal marsupials) and regional specialization in the vertebral column are required to interpret these results.

In terms of the platyrrhine taxa considered here, *Alouatta* showed stronger degrees of modularity in the axial skeleton, similar to that found in hominoids. In comparison, *Sapajus* showed similar degrees of modularity in the axial skeleton to cercopithecoids (Fig. 2; Table 2; SOM Tables S8 and S9). These differences among platyrrhine taxa may be related to differences in positional behaviors (i.e., locomotion and posture) and/or body size as atelids are the largest platyrrhines and *Alouatta* engage in bridging, suspensory, and climbing behaviors (Fleagle and Mittermeier, 1980; Fleagle, 2013). In contrast, capuchins are arboreal quadrupeds with body sizes similar to other cercopithecoids such as guenons (Fleagle and Mittermeier, 1980; Fleagle, 2013). For example, Fleagle and Mittermeier (1980) reported that *Alouatta seniculus* used suspensory behavior (including climbing) for 16% of travel and 41% of feeding behaviors. In comparison, suspensory behavior was used for 5% of travel and 8% of feeding behaviors in *Sapajus apella* and for 70% of travel and 73% of feeding behaviors in *Ateles paniscus* (Fleagle and Mittermeier, 1980). Johnson and Shapiro (1998) found that atelids showed similar vertebral morphology to hominoids,

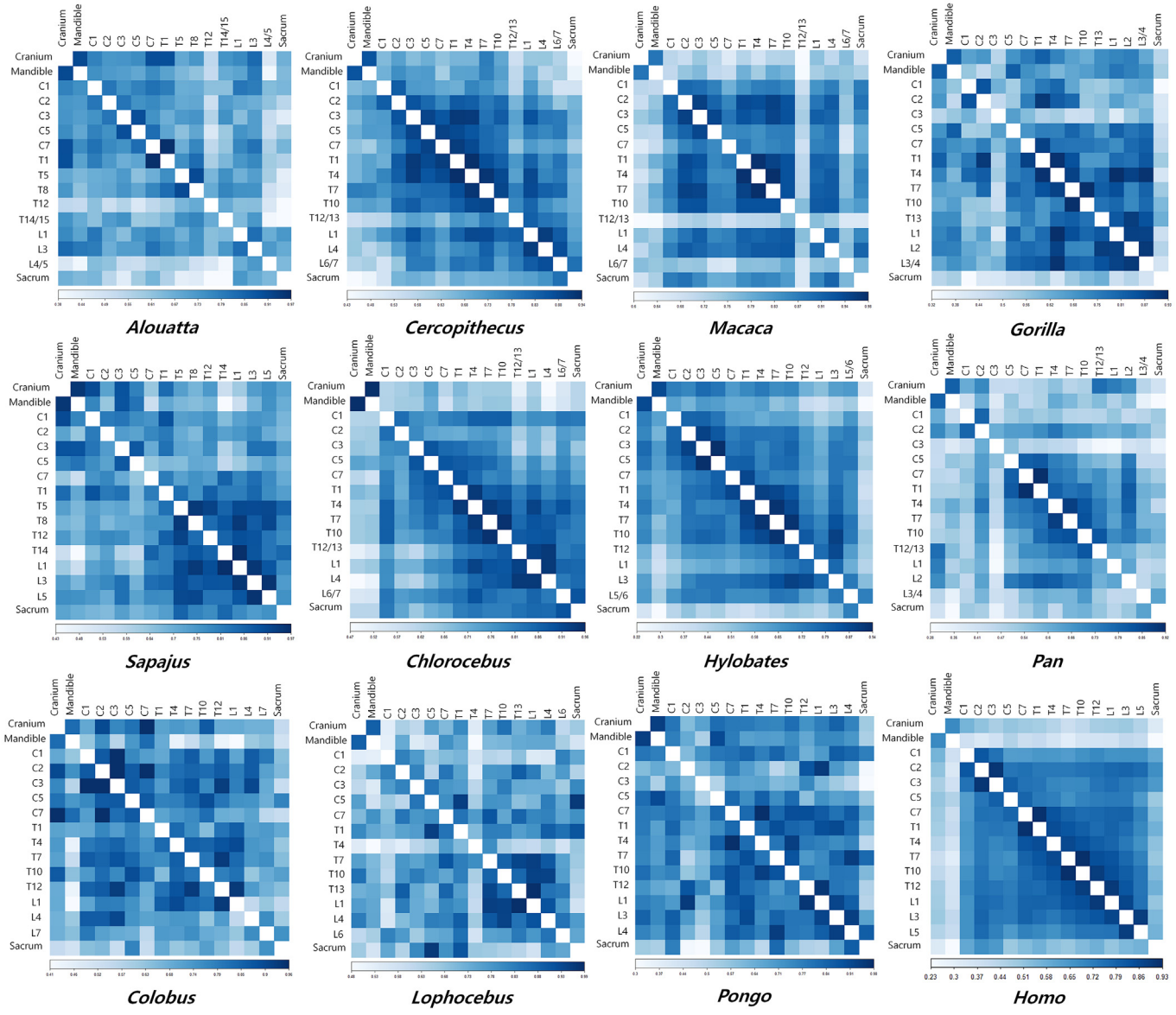

Figure 3. Heatmap of covariance ratio coefficient (CR) between axial skeletal elements. Diagonal elements are not included in the heatmap. Dark and light blue color represents relatively higher and lower CR values, respectively. (For interpretation of the references to color in this figure legend, the reader is referred to the Web version of this article.)

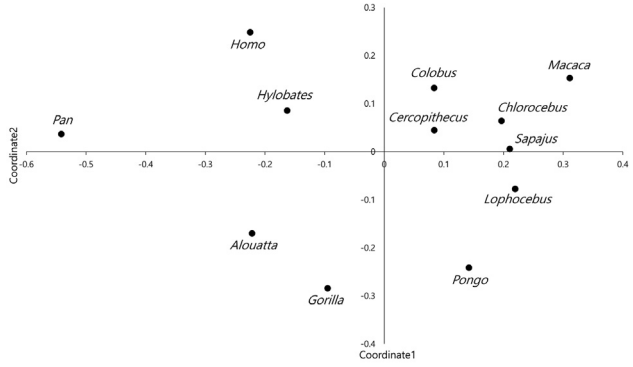

Figure 4. Bidimensional nonmetric multidimensional scaling plot of distance matrix of degrees of modularity in the axial skeletal elements as a whole ('stress' value = 0.1922).

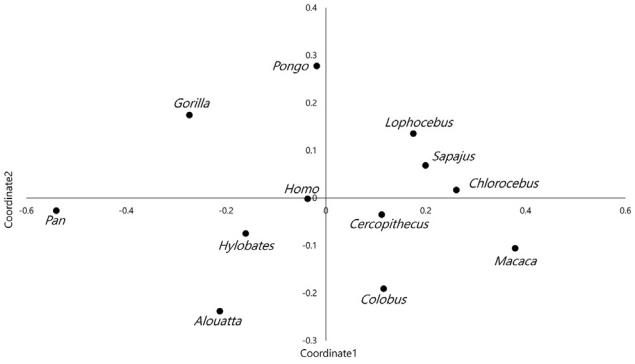

Figure 5. Bidimensional nonmetric multidimensional scaling plot of distance matrix of degrees of modularity in the vertebral elements as a whole ('stress' value = 0.1563).

such as more ventrodorsally elongated and craniocaudally shorter lumbar vertebral bodies. In contrast, capuchins show similar vertebral morphology to arboreal quadrupedal cercopithecoids, such as craniocaudally longer lumbar vertebral bodies (Johnson and Shapiro, 1998). *Alouatta* shows intermediate vertebral morphology between *Ateles* and *Cebus* as *Alouatta* use more arboreal quadrupedal locomotion than *Ateles* (Johnson and Shapiro, 1998). Thus, the results found here, whereby *Alouatta* is somewhat similar to hominoids, while *Sapajus* is similar to cercopithecoids, are most likely related to similarities in the biomechanical demands of positional behaviors, despite the lack of phylogenetic relatedness. Analyses that include more suspensory platyrrhine taxa (e.g., *Ateles* and *Brachyteles*) may allow for the effect of phylogenetic relatedness and convergent functional pressures on patterns of morphological modularity of the vertebral column to be parsed out.

The convergence in the degree of modularity between hominoids and *Alouatta* suggests the possibility that Miocene apes with more extant ape-like axial skeletal morphologies may have had relatively stronger degrees of modularity related to the functional demands of antipronograde (e.g., suspensory) positional behaviors. This inference is based on quantitative genetic models that predict morphological evolution and diversification in relation to novel functional pressures and/or function-induced increases in genetic and developmental modularity between serially homologous structures (Lande 1979; Cheverud 1996; Wagner and Altenberg, 1996; Hallgrímsson et al., 2002, 2009; Young and Hallgrímsson, 2005; Rolian, 2009, 2014; Young et al., 2010). As serially homologous structures, the axial skeletal elements (i.e., occipital region in the skull and vertebral column) share developmental factors in terms of somite differentiation and segregation from paraxial mesoderm regulated by common genetic pathways, such as the Hox gene family (Burke et al., 1995; Wellik, 2007). There are overlaps and distinctions in Hox gene expression domains between axial skeletal elements (Burke et al., 1995; Wellik, 2007), which may result in correlated responses to selection or relative independence between axial skeletal regions. Nevertheless, this does not suggest any specific developmental processes for establishing observed covariance structure, as covariances among traits cannot be attributed to specific developmental determinants as the generation of covariance structure is dependent on developmental processes that are superimposed during ontogeny (Hallgrímsson et al., 2009). The strong modularity of axial skeletal elements in hominoids and *Alouatta* suggest that there may have been changes in functional demands and ensuing genetic/developmental modularization (i.e., reduced constraints) in Miocene apes with more extant ape-like axial skeletal morphologies. Reduced developmental/genetic constraint in suspensory taxa is also reflected in variability in the number of presacral vertebrae, as there is higher variation in numbers of presacral vertebrae in suspensory (i.e., antipronograde) mammals, including hominoids, except for *Homo sapiens* and *Gorilla beringei* (Williams et al., 2019). The relative stability in the number of presacral vertebrae in the latter two taxa likely reflects adaptations for bipedalism or more terrestrial positional behaviors, respectively (Williams et al., 2019). It has been suggested that antipronograde and dorsostable positional behaviors reduce biomechanical and developmental (and genetic) constraints from dorsomobile activities, such as leaping and running (Williams et al., 2019). In other words, stabilizing selection on presacral vertebrae number may have been reduced in antipronograde and dorsostable mammals, including hominoids (Williams et al., 2019). Furthermore, Shapiro and Kemp (2019) reported that *Chlorocebus* generally had less variation in vertebral dimensions than hominoids, which also suggests that stabilizing selection may limit morphological variation in the vertebrae of pronograde and dorsomobile *Chlorocebus*. Some Early and Middle Miocene apes had more monkey-like torso and limb morphology reflecting generalized quadrupedalism, such as *Proconsul*, *Nacholapithecus*, *Equatorius*, and *Griphopithecus* (Ward, 1993, 2015; Kikuchi et al., 2015), whereas other Early and Middle Miocene apes such as *Morotopithecus* and *Pierolapithecus* (Sanders and Bodenbender, 1994; Nakatsukasa, 2008, 2019; Ward, 2015) and Late Miocene apes such as *Oreopithecus*, *Hispanopithecus*, and *Rudapithecus* (Russo and Shapiro, 2013; Susanna et al., 2014; Ward, 2015; but see Ward et al., 2019) exhibited more extant ape-like torso morphology with below-branch arboreal activities. Thus, the modularity results presented here suggest that Miocene apes with torso morphology more similar to extant apes had stronger degrees of modularity than those, such as *Proconsul*, with a more monkey-like torso morphology. Jung et al. (2021) also reported that *Hylobates*, *Pan*, and *Homo* generally showed weaker magnitudes of integration within each presacral vertebra than *Chlorocebus*, *Cercopithecus*, and *Macaca* although there were some exceptions. Thus, the present study and Jung et al. (2021) indicate there may have been weaker genetic constraints among traits or lower evolutionary constraint in the axial skeleton of Miocene apes with extant ape-like torso morphology in terms of morphological integration/modularity. It is worth noting that morphological modularity has not yet been quantified in extinct apes, and therefore, it is also possible that Miocene apes had stronger degrees of modularity in the axial skeleton than other anthropoids in general, despite variation in axial skeletal morphology and presumed positional behaviors. The only way to resolve this issue would be to directly measure the degrees of modularity in the axial skeletons of extinct Miocene apes in the future should a sufficient sample of fossilized axial skeletal data become available.

4.2. Implications for the evolution and diversification of hominin axial skeletal morphology

As predicted by the second hypothesis, humans showed different patterns of modularity than other hominoids (Fig. 3). In the case of vertebral elements, *Homo* exhibited a relatively high level of covariation compared with other hominoids, and was not significantly different from *Cercopithecus*, *Colobus*, and *Lophocebus* (Table 2; SOM Table S9). The heatmap showed more evenly patterned CR in the vertebral elements of *Homo* (Fig. 3), whereby sequential vertebral elements showed higher CR values than vertebrae further away. Moreover, *Homo* showed distinctive patterns of strong modularity, in terms of the relationship between the skull and the vertebral column, compared with other hominoids (Fig. 3; Table 2; SOM Tables S8–S10). Jung et al. (2021) showed that humans generally had weaker magnitudes of integration within each presacral vertebra than cercopithecoids, which suggests morphological traits within each vertebra may be more independently evolvable (i.e., weak magnitudes of integration within each vertebra) but morphological evolution is coordinated between vertebrae (i.e., strong covariation between sequential vertebral elements). Although not directly comparable to this study, ancestral state reconstruction of variability in the number of presacral vertebrae in the superfamily Hominoidea and between the Panini and Hominini tribes were also found to be close to antipronograde mammals (Williams et al., 2019). If we assume that the last common ancestor (LCA) of humans and chimpanzees had a more chimp-like morphotype (Pilbeam and Lieberman, 2017), the LCA may have had relatively stronger modularity (i.e., lower covariation) in vertebral elements as suggested by the results for *Pan* in this study. Then, the degrees of modularity increased (i.e., reversed) in certain vertebral elements but decreased between the skull and vertebrae of *Homo* from the LCA state in response to the evolution of obligate bipedal locomotion. Alternatively, it is possible that

stronger degrees of modularity may have evolved independently in the axial skeleton of *Hylobates*, *Pan*, and *Gorilla* as similar degrees of modularity were found between *Pongo* and cercopithecoids in the axial skeleton (Table 2; SOM Tables S8 and S9). In this regard, a future modularity study using *Gorilla beringei* may provide interesting insights as presacral vertebrae number is stable in *G. beringei* like other pronograde mammals in contrast to *Gorilla gorilla* (Williams et al., 2019), which was used in the present study. Moreover, further studies using more antipronograde mammals, including primates, need to be conducted to test whether there is stronger modularity in axial skeletal elements and/or vertebral elements as well as less developmental constraints on the number of presacral vertebrae (Williams et al., 2019).

Homo showed stronger degrees of modularity between the skull and vertebral column than other hominoids in this study (Fig. 3; SOM Table S10). Thus, the independent evolution of the novel characteristics of the human skull and vertebrae may have been facilitated by a decoupling of these elements in terms of trait covariance. If the skull and vertebral column experienced different strengths of selection and/or evolutionary rates in hominins, this stronger modularity may have allowed greater evolutionary independence for the skull and vertebral column to evolve in novel ways (see Klingenberg, 2014). Moreover, the results of this study suggest that fossil hominins may have had a mosaic of primitive and derived axial skeletal morphologies reflecting reduced constraint to paths of diversification in hominoid ancestors in terms of stronger degrees of modularity in the axial skeleton than other anthropoids.

5. Conclusions

In conclusion, the results of this study indicate that the overall stronger modularity of the hominoid axial skeleton may reflect less constraint in extinct and extant hominoids on the evolution of novel axial skeletal morphologies, as has previously been shown in limb bones (Young et al., 2010). Moreover, humans showed stronger modularity between the skull and vertebral elements than other hominoids. Thus, the results suggest a deep divergence (e.g., at the level of family/superfamily) in the modularity among skeletal elements between hominoids and other anthropoids, and between humans and other hominoids. Moreover, the convergence between hominoids and *Alouatta* suggests that stronger degrees of modularity in the axial skeleton are not a unique feature of hominoids among primates but may be shared with phylogenetically distant taxa with similar functional demands. The results also indicate the strong possibility that Miocene apes with extant ape-like vertebral morphologies and positional behaviors (i.e., locomotion and posture) may have had stronger degrees of modularity in the axial skeleton relative to more monkey-like Miocene apes, although this is difficult to measure directly due to small sample sizes of fragmentary fossil specimens. Further studies including more comparative primate and other mammalian taxa (e.g., spider monkeys, indri lemurs, and bipedal marsupials) will be essential to elaborate more comprehensive relationships between evolutionary independence (e.g., degrees of modularity), phylogenetic history, and positional behaviors in the axial skeleton.

Declaration of competing interest

None.

Acknowledgments

We thank the Editor-in-Chief, Associate Editor and three anonymous reviewers for their constructive comments on an earlier version of this paper. We are grateful to Yohannes Haile-Selassie at the Cleveland Museum of Natural History, Lawrence Heaney at the Field Museum of Natural History, Darrin Lunde at the Smithsonian Museum of Natural History, Mark Omura at the Museum of Comparative Zoology at the Harvard University, Dawnie Steadman at the Forensic Anthropology Center at the University of Tennessee-Knoxville, and staffs at the Neil C. Tappen Collection at the University of Minnesota and the American Museum of Natural History for granting access to skeletal materials for data collection. We thank the SUNY Reuter Foundation to support this research. This material is based upon work supported by the National Science Foundation under grant number BCS-1830745 and the Mark Diamond Research Fund of the Graduate Student Association at the University at Buffalo, the State University of New York.

Author contributions

H.J. contributed to conceptualization, data curation, formal analysis, investigation, visualization, and writing original draft. N.v.C.T. contributed to conceptualization, investigation, supervision, and funding acquisition. All authors contributed critically to the drafts and gave final approval for publication.

Supplementary Online Material

Supplementary Online Material related to this article can be found at https://doi.org/10.1016/j.jhevol.2022.103256.

References

Adams, D.C., 2016. Evaluating modularity in morphometric data: Challenges with the RV coefficient and a new test measure. Methods Ecol. Evol. 7, 565–572.
Adams, D.C., Otárola-Castillo, E., 2013. geomorph: an R package for the collection and analysis of geometric morphometric shape data. Methods Ecol. Evol. 4, 393–399.
Arlegi, M., Gómez-Robles, A., Gómez-Olivencia, A., 2018. Morphological integration in the gorilla, chimpanzee, and human neck. Am. J. Phys. Anthropol. 166, 408–416.
Arlegi, M., Veschambre-Couture, C., Gómez-Olivencia, A., 2020. Evolutionary selection and morphological integration in the vertebral column of modern humans. Am. J. Phys. Anthropol. 171, 17–36.
Arlegi, M., Pantoja-Pérez, A., Veschambre-Couture, C., Gómez-Olivencia, A., 2022. Covariation between the cranium and the cervical vertebrae in hominids. J. Hum. Evol. 162, 103112.
Armbruster, W.S., Pélabon, C., Bolstad, G.H., Hansen, T.F., 2014. Integrated phenotypes: Understanding trait covariation in plants and animals. Philos. Trans. R. Soc. B 369, 20130245.
Arsuaga, J.L., Carretero, J.M., Lorenzo, C., Gómez-Olivencia, A., Pablos, A., Rodríguez, L., García-González, R., Bonmatí, A., Quam, R.M., Pantoja-Pérez, A., Martínez, I., Aranburu, A., Gracia-Téllez, A., Poza-Rey, E., Sala, N., García, N., de Velasco, A.A., Cuenca-Bescós, G., Bermúdez de Castro, J.M., Carbonell, E., 2015. Postcranial morphology of the middle Pleistocene humans from Sima de los Huesos, Spain. Proc. Natl. Acad. Sci. USA 112, 11524–11529.
Been, E., Gómez-Olivencia, A., Kramer, P.A. (Eds.), 2019. Spinal Evolution: Morphology, Function, and Pathology of the Spine in Hominoid Evolution. Springer, Cham, Switzerland.
Burke, A.C., Nelson, C.E., Morgan, B.A., Tabin, C., 1995. *Hox* genes and the evolution of vertebrate axial morphology. Development 121, 333–346.
Cheverud, J.M., 1996. Developmental integration and the evolution of pleiotropy. Am. Zool. 36, 44–50.
Fleagle, J.G., 2013. Primate Adaptation and Evolution. Academic Press, New York.
Fleagle, J.G., Mittermeier, R.A., 1980. Locomotor behavior, body size, and comparative ecology of seven Surinam monkeys. Am. J. Phys. Anthropol. 52, 301–314.
Gómez-Olivencia, A., Been, E., Arsuaga, J.L., Stock, J.T., 2013. The Neandertal vertebral column 1: The cervical spine. J. Hum. Evol. 64, 608–630.
Gómez-Olivencia, A., Arlegi, M., Barash, A., Stock, J.T., Been, E., 2017. The Neandertal vertebral column 2: The lumbar spine. J. Hum. Evol. 106, 84–101.
Gómez-Olivencia, A., Been, E., 2019. The spine of late Homo. In: Been, E., Gómez-Olivencia, A., Kramer, P. (Eds.), Spinal Evolution: Morphology, Function, and Pathology of the Spine in Hominoid Evolution. Springer, Cham, pp. 185–211.
Gómez-Robles, A., Smaers, J.B., Holloway, R.L., Polly, P.D., Wood, B.A., 2017. Brain enlargement and dental reduction were not linked in hominin evolution. Proc. Natl. Acad. Sci. USA 114, 468–473.

Goswami, A., Smaers, J.B., Soligo, C., Polly, P.D., 2014. The macroevolutionary consequences of phenotypic integration: From development to deep time. Philos. Trans. R. Soc. B 369, 20130254.
Groenen, P.J., van de Velden, M., 2005. Multidimensional scaling. In: Everitt, B.S., Howell, D.C. (Eds.), Encyclopedia of Statistics in Behavioral Science. John Wiley & Sons, Ltd, Chichester, pp. 1280–1289.
Hallgrímsson, B., Willmore, K., Hall, B.K., 2002. Canalization, developmental stability, and morphological integration in primate limbs. Am. J. Phys. Anthropol. 119, 131–158.
Hallgrímsson, B., Jamniczky, H., Young, N.M., Rolian, C., Parsons, T.E., Boughner, J.C., Marcucio, R.S., 2009. Deciphering the palimpsest: Studying the relationship between morphological integration and phenotypic covariation. Evol. Biol. 36, 355–376.
Hammer, Ø., Harper, D.A., Ryan, P.D., 2001. PAST: Paleontological statistics software package for education and data analysis. Palaeontol. Electron. 4, 9.
Iacobucci, D., Schneider, M.J., Popovich, D.L., Bakamitsos, G.A., 2016. Mean centering helps alleviate "micro" but not "macro" multicollinearity. Behav. Res. Methods 48, 1308–1317.
Johanson, D.C., Lovejoy, C.O., Kimbel, W.H., White, T.D., Ward, S.C., Bush, M.E., Latimer, B.M., Coppens, Y., 1982. Morphology of the Pliocene partial hominid skeleton (AL 288-1) from the Hadar formation, Ethiopia. Am. J. Phys. Anthropol. 57, 403–451.
Johnson, S.E., Shapiro, L.J., 1998. Positional behavior and vertebral morphology in atelines and cebines. Am. J. Phys. Anthropol. 105, 333–354.
Jones, K.E., Angielczyk, K.D., Polly, P.D., Head, J.J., Fernandez, V., Lungmus, J.K., Tulga, S., Pierce, S.E., 2018. Fossils reveal the complex evolutionary history of the mammalian regionalized spine. Science 361, 1249–1252.
Jung, H., Simons, E.A., von Cramon-Taubadel, N., 2021. Examination of magnitudes of integration in the catarrhine vertebral column. J. Hum. Evol. 156, 102998.
Kikuchi, Y., Nakatsukasa, M., Nakano, Y., Kunimatsu, Y., Shimizu, D., Ogihara, N., Tsujikawa, H., Takano, T., Ishida, H., 2015. Morphology of the thoracolumbar spine of the middle Miocene hominoid *Nacholapithecus kerioi* from northern Kenya. J. Hum. Evol. 88, 25–42.
Klingenberg, C.P., 2014. Studying morphological integration and modularity at multiple levels: Concepts and analysis. Philos. Trans. R. Soc. B 369, 20130249.
Lande, R., 1979. Quantitative genetic analysis of multivariate evolution, applied to brain: Body size allometry. Evolution 33, 402–416.
Latimer, B., Ward, C.V., 1993. The thoracic and lumbar vertebrae. In: Walker, A., Leakey, R. (Eds.), The Nariokotome *Homo erectus* Skeleton. Harvard University Press, Cambridge, pp. 267–293.
Lieberman, D., 2011. The Evolution of the Human Head. Harvard University Press, Cambridge.
Lieberman, D.E., Ross, C.F., Ravosa, M.J., 2000. The primate cranial base: Ontogeny, function, and integration. Am. J. Phys. Anthropol. 113, 117–169.
Lovejoy, C.O., Johanson, D.C., Coppens, Y., 1982. Hominid lower limb bones recovered from the Hadar Formation: 1974–1977 collections. Am. J. Phys. Anthropol. 57, 679–700.
Meyer, M.R., 2005. Functional biology of the *Homo erectus* axial skeleton from Dmanisi. Ph.D. Dissertation, University of Pennsylvania, Georgia.
Meyer, M.R., Williams, S.A., Smith, M.P., Sawyer, G.J., 2015. Lucy's back: Reassessment of fossils associated with the AL 288-1 vertebral column. J. Hum. Evol. 85, 174–180.
Meyer, M.R., Williams, S.A., Schmid, P., Churchill, S.E., Berger, L.R., 2017. The cervical spine of *Australopithecus sediba*. J. Hum. Evol. 104, 32–49.
Meyer, M.R., Williams, S.A., 2019. The spine of early Pleistocene Homo. In: Been, E., Gómez-Olivencia, A., Kramer, P. (Eds.), Spinal Evolution: Morphology, Function, and Pathology of the Spine in Hominoid Evolution. Springer, Cham, pp. 153–183.
Nakatsukasa, M., 2008. Comparative study of Moroto vertebral specimens. J. Hum. Evol. 55, 581–588.
Nakatsukasa, M., 2019. Miocene ape spinal morphology: The evolution of orthogrady. In: Been, E., Gómez-Olivencia, A., Kramer, P. (Eds.), Spinal Evolution: Morphology, Function, and Pathology of the Spine in Hominoid Evolution. Springer, Cham, pp. 73–96.
Neaux, D., Sansalone, G., Ledogar, J.A., Ledogar, S.H., Luk, T.H., Wroe, S., 2018. Basicranium and face: Assessing the impact of morphological integration on primate evolution. J. Hum. Evol. 118, 43–55.
Pilbeam, D.R., Lieberman, D.E., 2017. Reconstructing the last common ancestor of chimpanzees and humans. In: Muller, M.N., Wrangham, R.W., Pilbeam, D.R. (Eds.), Chimpanzees and Human Evolution. Harvard University Press, Cambridge, pp. 22–141.
R Core Team, 2020. R: A language and environment for statistical computing. R Foundation for Statistical Computing, Vienna, Austria. URL: http://www.R-project.org/.
Randau, M., Goswami, A., 2017. Morphological modularity in the vertebral column of Felidae (Mammalia, Carnivora). BMC Evol. Biol. 17, 1–12.
Rolian, C., 2009. Integration and evolvability in primate hands and feet. Evol. Biol. 36, 100–117.
Rolian, C., 2014. Genes, development, and evolvability in primate evolution. Evol. Anthropol. 23, 93–104.
Russo, G.A., Shapiro, L.J., 2013. Reevaluation of the lumbosacral region of *Oreopithecus bambolii*. J. Hum. Evol. 65, 253–265.
Russo, G.A., Williams, S.A., 2015. Lucy" (A.L. 288-1) had five sacral vertebrae. Am. J. Phys. Anthropol. 156, 295–303.
Sanders, W.J., Bodenbender, B.E., 1994. Morphometric analysis of lumbar vertebra UMP 67-28: Implications for spinal function and phylogeny of the Miocene Moroto hominoid. J. Hum. Evol. 26, 203–237.
Schroeder, L., von Cramon-Taubadel, N., 2017. The evolution of hominoid cranial diversity: A quantitative genetic approach. Evolution 71, 2634–2649.
Shapiro, L.J., 1993a. Functional morphology of the vertebral column in primates. In: Gebo, D.L. (Ed.), Postcranial Adaptation in Non-human Primates. Northern Illinois University, Dekalb, pp. 121–149. Press.
Shapiro, L., 1993b. Evaluation of "unique" aspects of human vertebral bodies and pedicles with a consideration of *Australopithecus africanus*. J. Hum. Evol. 25, 433–470.
Shapiro, L.J., Kemp, A.D., 2019. Functional and developmental influences on intraspecific variation in catarrhine vertebrae. Am. J. Phys. Anthropol. 168, 131–144.
Susanna, I., Alba, D.M., Almécija, S., Moya-Sola, S., 2014. The vertebral remains of the late Miocene great ape *Hispanopithecus laietanus* from can Llobateres 2 (Vallès-Penedès Basin, NE Iberian Peninsula). J. Hum. Evol. 73, 15–34.
Veneziano, A., Meloro, C., Irish, J.D., Stringer, C., Profico, A., De Groote, I., 2018. Neuromandibular integration in humans and chimpanzees: Implications for dental and mandibular reduction in *Homo*. Am. J. Phys. Anthropol. 167, 84–96.
Villamil, C.I., 2018. Phenotypic integration of the cervical vertebrae in the Hominoidea (Primates). Evolution 72, 490–517.
Villamil, C.I., Santiago-Nazario, A., 2021. Integration between the cranial boundaries of the nasopharynx and the upper cervical vertebrae in *Homo* and *Pan*. Anat. Rec. 305, 1974–1990.
von Cramon-Taubadel, N., Frazier, B.C., Lahr, M.M., 2007. The problem of assessing landmark error in geometric morphometrics: Theory, methods, and modifications. Am. J. Phys. Anthropol. 134, 24–35.
von Cramon-Taubadel, N., Scott, J.E., Robinson, C.A., Schroeder, L., 2021. The evolution of the human chin: A quantitative genetic analysis of hominoid craniomandibular form. Am. J. Phys. Anthropol. 168, 109–110.
Wagner, G.P., Altenberg, L., 1996. Perspective: Complex adaptations and the evolution of evolvability. Evolution 50, 967–976.
Ward, C.V., 1993. Torso morphology and locomotion in *Proconsul nyanzae*. Am. J. Phys. Anthropol. 92, 291–328.
Ward, C.V., 2015. Postcranial and locomotor adaptations of hominoids. In: Tattersall, I., Henke, W. (Eds.), Handbook of Paleoanthropology. Springer, Berlin, pp. 1363–1386.
Ward, C.V., Hammond, A.S., Plavcan, J.M., Begun, D.R., 2019. A late Miocene hominid partial pelvis from Hungary. J. Hum. Evol. 136, 102645.
Wei, T., Simko, V., Levy, M., Xie, Y., Jin, Y., Zemla, J., 2017. Package 'corrplot. Statistician 56, e24.
Wellik, D.M., 2007. *Hox* patterning of the vertebrate axial skeleton. Dev. Dyn. 236, 2454–2463.
Wiley, D.F., Amenta, N., Alcantara, D.A., Ghosh, D., Kil, Y.J., Delson, E., Harcourt-Smith, W., Rohlf, F.J., Katherine, S.J., Hamann, B., 2005. Evolutionary morphing. https://escholarship.org/uc/item/4k5991zk.
Williams, S.A., Middleton, E.R., Villamil, C.I., Shattuck, M.R., 2016. Vertebral numbers and human evolution. Am. J. Phys. Anthropol. 159, 19–36.
Williams, S.A., Garcia-Martinez, D., Bastir, M., Meyer, M.R., Nalla, S., Hawks, J., Schmid, P., Churchill, S.E., Berger, L.R., 2017. The vertebrae and ribs of *Homo naledi*. J. Hum. Evol. 104, 136–154.
Williams, S.A., Meyer, M.R., Nalla, S., García-Martínez, D., Nalley, T.K., Eyre, J., Prang, T.C., Bastir, M., Schmid, P., Churchill, S.E., Berger, L.R., 2018. *Australopithecus sediba* – the vertebrae, ribs, and Sternum of *Australopithecus sediba*. PaleoAnthropology 2018, 156–233.
Williams, S.A., Meyer, M.R., 2019. The spine of Australopithecus. In: Been, E., Gómez-Olivencia, A., Kramer, P. (Eds.), Spinal Evolution: Morphology, Function, and Pathology of the Spine in Hominoid Evolution. Springer, Cham, pp. 125–151.
Williams, S.A., Spear, J.K., Petrullo, L., Goldstein, D.M., Lee, A.B., Peterson, A.L., Miano, D.A., Kaczmarek, E.B., Shattuck, M.R., 2019. Increased variation in numbers of presacral vertebrae in suspensory mammals. Nat. Ecol. Evol. 3, 949–956.
Williams, S.A., Prang, T.C., Meyer, M.R., Nalley, T.K., Van Der Merwe, R., Yelverton, C., García-Martínez, D., Russo, G.A., Ostrofsky, K.R., Spear, J., Eyre, J., Grabowski, M., Nalla, S., Bastir, M., Schmid, P., Churchill, S.E., Berger, L.R., 2021. New fossils of *Australopithecus sediba* reveal a nearly complete lower back. eLife 10, e70447.
Williams, S.A., Zeng, I., Paton, G.J., Yelverton, C., Dunham, C., Ostrofsky, K.R., Shukman, S., Avilez, M.V., Eyre, J., Loewen, T., Prang, T.C., Meyer, M.R., 2022. Inferring lumbar lordosis in Neandertals and other hominins. PNAS Nexus 1, pgab005.
Young, N.M., Hallgrímsson, B., 2005. Serial homology and the evolution of mammalian limb covariation structure. Evolution 59, 2691–2704.
Young, N.M., Wagner, G.P., Hallgrímsson, B., 2010. Development and the evolvability of human limbs. Proc. Natl. Acad. Sci. USA 107, 3400–3405.